Phys. Status Solidi B **246**, No. 9, 2025–2032 (2009) / **DOI** 10.1002/pssb.200982033

physica status solidi b
www.pss-b.com
basic solid state physics

On the effect of the Poisson's ratio (positive and negative) on the stability of pressure vessel heads

Brian Ellul[1], **Martin Muscat**[2], **and Joseph N. Grima**[*,1]

[1] Faculty of Science, University of Malta, Msida MSD 2080, Malta
[2] Faculty of Engineering, University of Malta, Msida MSD 2080, Malta

Received 18 March 2009, revised 25 May 2009, accepted 25 May 2009
Published online 12 August 2009

PACS 62.20.−x, 62.20.dj, 62.20.mq, 62.50.−p

* Corresponding author: e-mail joseph.grima@um.edu.mt, Phone: +00 356 2340 2274, Fax: +00 356 2133 0400

Materials with negative Poisson's ratio (auxetic) exhibit an unusual property of expanding when stretched in the direction normal to an applied uniaxial tension and *vice versa* when compressed, a phenomenon which is known to result in many beneficial effects in the performance of materials in various practical situations. In particular, it has long been suggested that spherical shells made from isotropic materials having Poisson's ratio less than −0.5 exhibit enhanced resistance to buckling as a result of externally applied normal pressure. This work uses finite elements (FEs) modelling to assess the behaviour of various spherical, torispherical and ellipsoidal shells when they are subjected to external (in all cases) or internal (in the case of torispherical and ellipsoidal shells) pressures. We find that to a first approximation, the critical buckling pressures scale linearly with $(1-\nu^2)^{-1/2}$ thus suggesting that the critical buckling pressures tends to infinity as ν tends to −1, this being in accordance to what was known for spherical shells. We also find that the Poisson's ratio has an effect on the amplitude and the number of buckling wavelengths that occur when the shells buckle.

1 Introduction Materials with negative Poisson's ratio, ν, also known as auxetic materials, have an unusual property of getting fatter when stretched and thinner when compressed. Varying the Poisson's ratio of a material below zero, is a relatively new concept in the engineering field, although elastic theory predicts that for isotropic materials, ν can vary between −1 and 0.5. However, in recent years, several studies have been conducted, with the result that a number of auxetics have now been predicted, discovered and/or manufactured [1–37]. Furthermore, various theoretical and/or experimental studies have shown that auxetics exhibit several enhanced characteristics ranging from having a natural ability to form dome-shaped surfaces as opposed to saddle shaped surfaces [3] and increased vibration absorption [4]. Nevertheless, there are still various engineering applications which could benefit from having auxetic materials, which still need to be investigated in detail. Such is the design of smart structures which offer greater resistance to buckling (structural instability).

Buckling usually occurs in thin/slender structures subjected to compressive stresses and failure occurs at a lower load with respect to the material's ultimate compressive strength. The Swiss mathematician and physicist, Leonhard Euler (1707–1783), published a paper on column buckling where he showed that slender columns under axial compression failed due to their slender geometry rather than material failure alone. Since then, the subject was extensively researched, *e.g.* analytically, experimentally and numerically [36–47]. For example, buckling is one type of failure that pressure vessel designers must take into account when designing thin shell containers subjected to either internal or external pressures. In such systems, structural instability occurs due to the fact that certain shell geometries, such as a torisphere (Fig. 1b) which is a shape made of a spherical central portion of radius R_s and a toroidal knuckle of radius R_t, develop compressive hoop stresses in certain regions [48], as a result of an applied surface pressure. A structure which has been studied extensively is the sphere

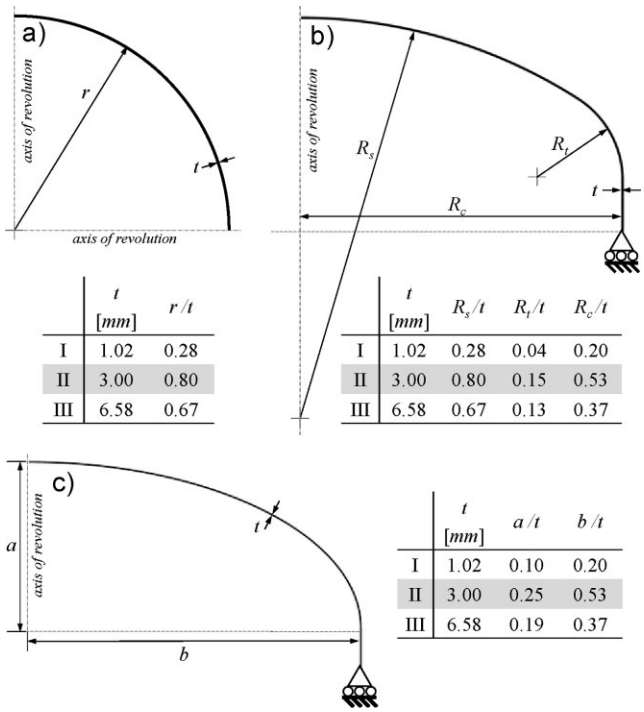

	t [mm]	r/t
I	1.02	0.28
II	3.00	0.80
III	6.58	0.67

	t [mm]	R_s/t	R_t/t	R_c/t
I	1.02	0.28	0.04	0.20
II	3.00	0.80	0.15	0.53
III	6.58	0.67	0.13	0.37

	t [mm]	a/t	b/t
I	1.02	0.10	0.20
II	3.00	0.25	0.53
III	6.58	0.19	0.37

Figure 1 Dimensions of the (a) spheres, (b) torispheres and (c) ellipsoids analysed.

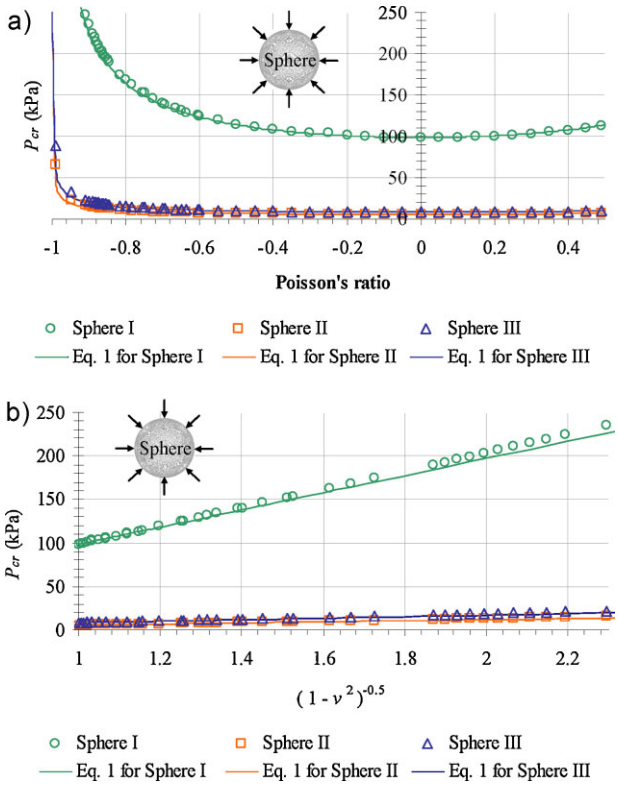

Figure 2 (online colour at: www.pss-b.com) Plots of the variation of the critical buckling pressure P_{cr} with (a) the Poisson's ratio ν and (b) the $(1-\nu^2)^{-1/2}$ fraction together with a linear regression of the form $y = mx + c$.

which buckles under external pressure. In this respect, we note that [49, 50] showed that the critical elastic buckling pressure (P_{cr}) for a spherical shell made from an isotropic material, subjected to a uniform external normal pressure, is given by:

$$P_{cr} = \frac{2E}{\sqrt{3}} \left(\frac{t}{r}\right)^2 \left(1-\nu^2\right)^{-1/2}, \qquad (1)$$

where t is the thickness of the shell, r the radius of the shell, E the Young's Modulus and ν is the Poisson's ratio of the material. This equation suggests that the critical buckling pressure is highly dependent on the Poisson's ratio of the material and this dependence becomes more significant for auxetic materials as ν tends to -1 when the critical buckling pressure for a sphere will tend to infinity. This suggests that auxetic shells can exhibit significant increased buckling resistance (Fig. 2a) when compared to shells made of material having a positive Poisson's ratio. Note that spheres I, II and III refer to the corresponding dimensions listed in Fig. 1. More recently, similar enhanced characteristics were observed by Obrecht et al. [51]. Using finite element (FE) modelling Obrecht et al. have shown that when a thin cylindrical shell and a plate are subjected to different types of loadings one would observe an enhancement in the buckling resistance for auxetic systems as the Poisson's ratio approaches the value of -1.

Analytical equations such as Eq. (1) which predict the critical elastic buckling pressure as a function of several material and structural properties including the Poisson's ratio, only exist for very simple geometries such as cylinders and spheres. To the authors' knowledge, no such mathematical models exist for more complex shapes such as torispheres and ellipsoids which are more commonly used in practical engineering applications.

This paper examines through linear FE modelling the effect of the Poisson's ratio on the properties of thin shells of various geometrical shapes usually used as pressure vessel heads. In particular we examine whether FE modelling results can reproduce the predictions by [49, 50], in particular whether an ideal (*i.e.* without defects) spherical shell made from isotropic materials exhibits enhanced stability properties, when the ν is negative and lower than -0.5. This work further investigates whether non-spherical torispherical and ellipsoidal pressure vessel heads (two shapes which are commonly used as ends in pressure vessels) made from isotropic materials will also exhibit similar enhancement.

2 Methodology Numerical analysis aimed at studying the effect of the Poisson's ratio on the buckling mode and on the critical buckling pressure of the thin spherical, torispherical and elliptical shells under uniform external (in all cases) and internal (in the case of the torispherical and elliptic shells only) pressure were performed using the FEs software ANSYS® [52]. The FE matrix formulation for solving a linear buckling analysis which in turn is an

eigenvalue problem of the form:

$$[K]\{\boldsymbol{u}\} + \lambda [N]\{\boldsymbol{u}\} = 0, \tag{2}$$

where $[K]$ is the stiffness matrix, $[N]$ the load geometric matrix while $\{\boldsymbol{u}\}$ and λ are the eigenvector and eigenvalue, respectively which correspond to the buckling mode and the critical buckling pressure. The $[N]$ matrix is assembled based on the stress state of each element of the structure, which is generated by an externally applied unit load. As in any other eigenvalue problem there can be multiple solutions for this problem thus implying that multiple eigenvectors/eigenvalues exist where usually the lowest (first) eigenvalue and eigenvector are considered as the critical ones, *i.e.* the ones which have the highest probability of occurring first.

To reduce computational requirements in each case, a quarter of the shell was modelled in 3D and meshed with the 4-noded SHELL63 elastic element together with appropriate symmetric boundary conditions to simulate a whole shell. The spheres, torispheres and ellipsoids were map meshed with ~19 000, 7400 and 30 800 elements, respectively, which mesh sizes were found to be fine enough to ensure convergence of the results obtained and also ensure smooth buckling modes.

In particular, every shell was modelled with three different sets of dimensions (henceforth referred to as I, II and III) as detailed in Fig. 1. The dimensions used for the torispheres were taken from [52–55] so as to analyse real world pressure vessel heads dimensions. The diameters of the cylindrical part of the other shells, *i.e.* the main cylindrical part of the vessel, was kept constant while the height of the ellipsoids was made equal to that of the torispheres. Note that in the simulations of the torispherical and ellipsoidal heads, the cylindrical parts were made thicker than the heads so as to ensure that in all cases, the heads of the pressure vessels buckle before the cylindrical part, *i.e.* the critical buckling pressure measured corresponds to buckling of the heads of the pressure vessels (the subject of this paper) rather than buckling of the cylindrical parts.

In all cases, the material chosen was isotropic perfectly elastic with a Young's modulus $E = 3.28$ GPa (the value of typical rigid PVC used in [55]) while the Poisson's ratio was given values within the range of $-1 < \nu < +0.5$.

3 The effect of the Poisson's ratio on the critical buckling pressure of spherical shells Plots of the critical buckling pressure (P_{cr}) against the Poisson's ratio of the material for the three spheres can be found in Fig. 2a where they are also compared to the predicted values of P_{cr} using Eq. (1). Shown in Fig. 2b are plots of P_{cr} against $(1-\nu^2)^{-1/2}$ (which are predicted by Eq. (1) to be linear with zero intercept) whilst a plot of the percentage difference between P_{cr} as simulated in ANSYS and P_{cr} as predicted by Eq. (1) is shown in Fig. 3.

These results clearly confirm that, to a first approximation, the FE simulations agree with the predictions made by Eq. (1) and in particular confirm, to a first approximation,

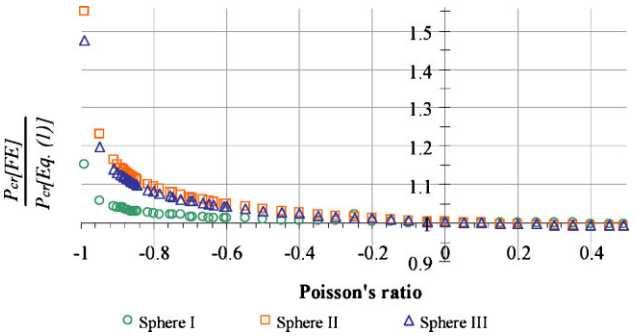

Figure 3 (online colour at: www.pss-b.com) Plots of the ratio between the critical buckling pressure given by the FE P_{cr}[FE] and the theoretical one P_{cr} [Eq. (1)].

a linear relationship with zero intercept between the critical bucking pressure P_{cr} and $(1-\nu^2)^{-1/2}$. Although no improvement is observed when the Poisson's ratio is in the range of -0.5 to 0 when compared to the positive Poisson's ratio region $0 < \nu < 0.5$. All this confirms that in the case of spherical shells the critical buckling pressure increases drastically as ν decreases further than –0.5. However, as illustrated in Fig. 3, on closer inspection of the results, we note that the FE simulations and the analytical expression given by Eq. (1) agree best when the Poisson's ratio is zero. For non-zero Poisson's ratio systems, the FE simulations result in a buckling pressure, which is lower than that predicted by the analytical model for shells made from conventional materials and higher in the case of auxetic shells. Figure 3 also suggests that the deviation increases as the Poisson's ratio decreases. This indicates that there is better agreement between Eq. (1) and the results of the FE simulation for systems where the Poisson's ratios are positive then when they are negative. In particular, for values of the Poisson's ratio where $\nu < -0.5$ (*i.e.* in the range of Poisson's ratio where one finds the enhancement of the resistance to buckling as a result of auxeticity), there is significant disagreement between the results of the simulations and the predictions made by Eq. (1) where the FE simulations suggests higher resistance to buckling than that predicted by Eq. (1).

In view of all this, Table 1 summarises the results of linear regression analyses between the critical buckling pressure and $(1-\nu^2)^{-1/2}$ for the data split in three regions: $0 \le \nu < +0.5$, $-0.5 \le \nu \le 0$ and $-1 < \nu \le -0.5$. The table lists the gradients (m), y-intercepts (c), the R-squared values (R^2) and the number of data points considered (n) for two types of linear regressions the first with zero intercept ($c = 0$) and the second with an intercept at $y = c$.

These results confirm that to a first approximation, one may assume a linear relationship with zero intercept between the critical bucking pressures $(1-\nu^2)^{-1/2}$ with best regression being observed in the region $0 \le \nu < +0.5$ where the data are in excellent agreement with Eq. (1). This is very significant as it gives confidence to the quality of the FE simulated results. At the same time this confirms the importance of carrying out such simulations for auxetic

Table 1 Linear regression analysis of P_{cr} with $(1-\nu^2)^{-1/2}$ for various regions of ν for the spherical shells compared with the theoretical one Note that linear regression analysis is performed first with zero intercept ($c=0$, *i.e.* $y=mx$) and the second with an intercept at $y=c$ (*i.e.* $y=mx+c$).

Set	ν	m	R^2	m	c	R^2	n
I	theory	98 511	–	98 511	–	–	–
	0 to 0.5	98 406	0.9995	96 445	2062	0.9999	11
	−0.5 to 0	99 100	0.9877	103 135	−4247	0.9892	11
	−1.0 to −0.5	105 788	0.9893	115 610	−24713	0.9986	30
II	theory	5918	–	5918	–	–	–
	0 to 0.5	5892	0.9934	5499	414	0.9986	11
	−0.5 to 0	6025	0.9660	7367	−1413	0.9993	11
	−1.0 to −0.5	7522	0.9301	9630	−5304	0.9916	30
III	theory	8509	–	8509	–	–	–
	0 to 0.5	8480	0.9954	8001	504	0.9990	11
	−0.5 to 0	8645	0.9732	10 312	−1756	0.9994	11
	−1.0 to −0.5	7522	0.9301	13 109	−6569	0.9930	30

systems and not rely solely on predictions extracted from expressions, which were originally derived for describing the behaviour of conventional systems. However, in this respect, it is important to emphasise that all FE work reported here was performed using linear analyses (*i.e.* assuming a linear stress–strain curve for the material) whilst in real systems one would expect significant non-linear effects in the material stress–strain data, especially at high strains such as the ones present when buckling occurs. In other words, although there are variations between the data predicted by the FE simulations when compared to the data predicted by Eq. (1), one would expect even higher variations as a result of non-linear effects and thus, it must be emphasised that all results reported and interpreted here should only be taken as an rough indicative guide of how a real auxetic material would behave rather than an absolute prediction.

4 The effect of the Poisson's ratio on the critical buckling pressure of non-spherical shells Plots of the critical buckling pressure against the Poisson's ratio of the material for the three torispheres and the three ellipsoids under positive and negative external pressures can be found in Fig. 4.

Also shown in Fig. 5 are plots of P_{cr} against $(1-\nu^2)^{-1/2}$ which data are fitted to linear equation of the form $y=mx+c$ where the results of the regression analysis are summarised in Tables 2–5.

These results clearly suggest that the critical buckling pressure for systems under an internal pressure is always simulated to be significantly higher that that for an external pressure, in accordance with common expectation. They also suggest that for all shapes, the simulated critical buckling pressure was found to vary linearly (to a first approximation) with $(1-\nu^2)^{-1/2}$ where in some cases the y-intercept is significant. All this suggests that although Eq. (1) is only applicable to perfect spheres, the $(1-\nu^2)^{-1/2}$ factor still applies to all the shells analysed in this paper. This is very significant as it clearly illustrates the advantages that arise for all forms of pressure vessels analysed here should they be manufactured from auxetic materials where the Poisson's ratio is lower than –0.5. In practice, this result suggests that it may be possible to manufacture such pressure heads from thinner plates, this being an important consideration in applications where weight of the pressure vessel needs to be minimised, *e.g.* in space or aeronautical applications. Of particular significance is also the fact that auxetic materials benefit from a natural ability to form dome shaped surfaces with the consequence that such curved surfaces of pressure vessels are likely to be easier to manufacture from auxetic plates when compared to plates made from conventional materials.

5 The effect of the Poisson's ratio on the shape of buckled structures It is well known that when buckling occurs, ideal spherical shells develop uniform bulges over the surface. Ideal torispherical and ellipsoidal shells can attain deformations in the form of axisymmetric or circumferential waves. This depends on the stress field which is in turn dependent, amongst other factors, on the actual geometry of the system, boundary conditions and the type of loading being applied. Our simulations on spherical, torispherical and ellipsoidal shells were consistent with this as illustrated in Fig. 6. In particular we note that in the case of the sphere, a series of waves crossing each other were formed due to the even distribution of compressive stresses; in the case where the ellipsoid is loaded externally, the buckling mode was axisymmetric while in the remaining cases, *i.e.* the ellipsoids under external pressure and the torisphere, a series of circumferential waves formed at the geometric discontinuity.

The results illustrated in Fig. 6 also clearly show that the Poisson's ratio does not seem to effect the buckling mode of the systems analysed here, but it has an effect on the number of wavelengths that form and the transverse displacements/amplitude. This effect is clearly illustrated in Table 6 which lists the number of circumferential buckling

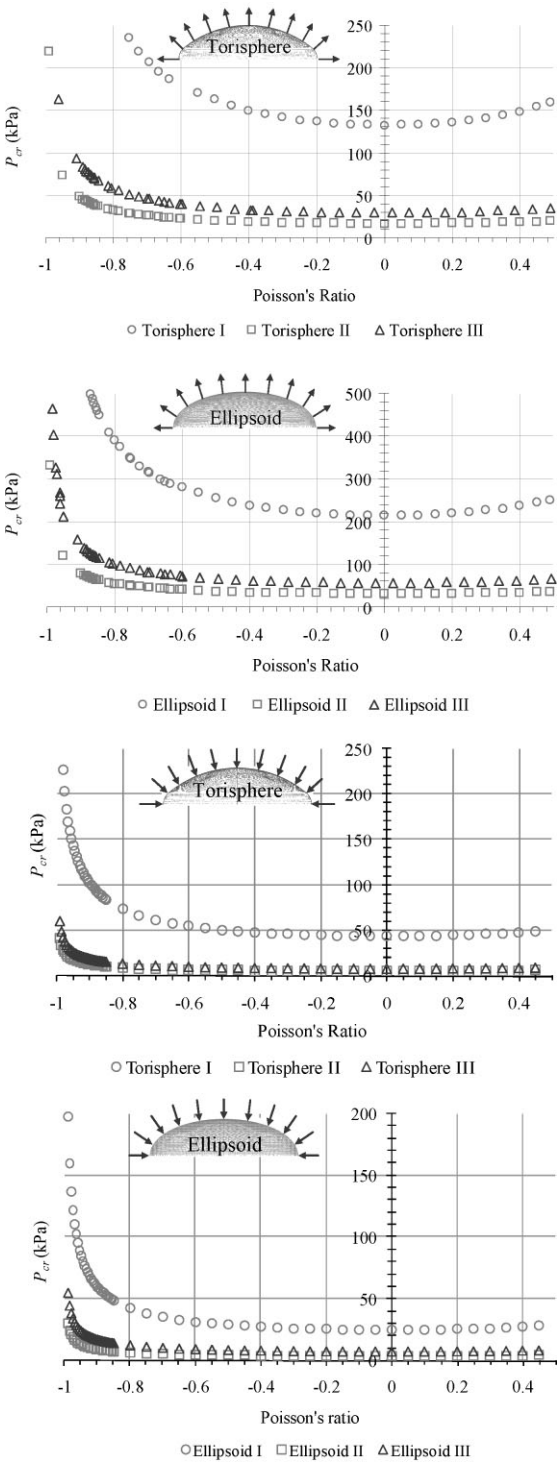

Figure 4 Plots showing the effect of the Poisson's ratio on the critical buckling pressure of the torispherical and ellipsoidal heads applied according to the diagrams.

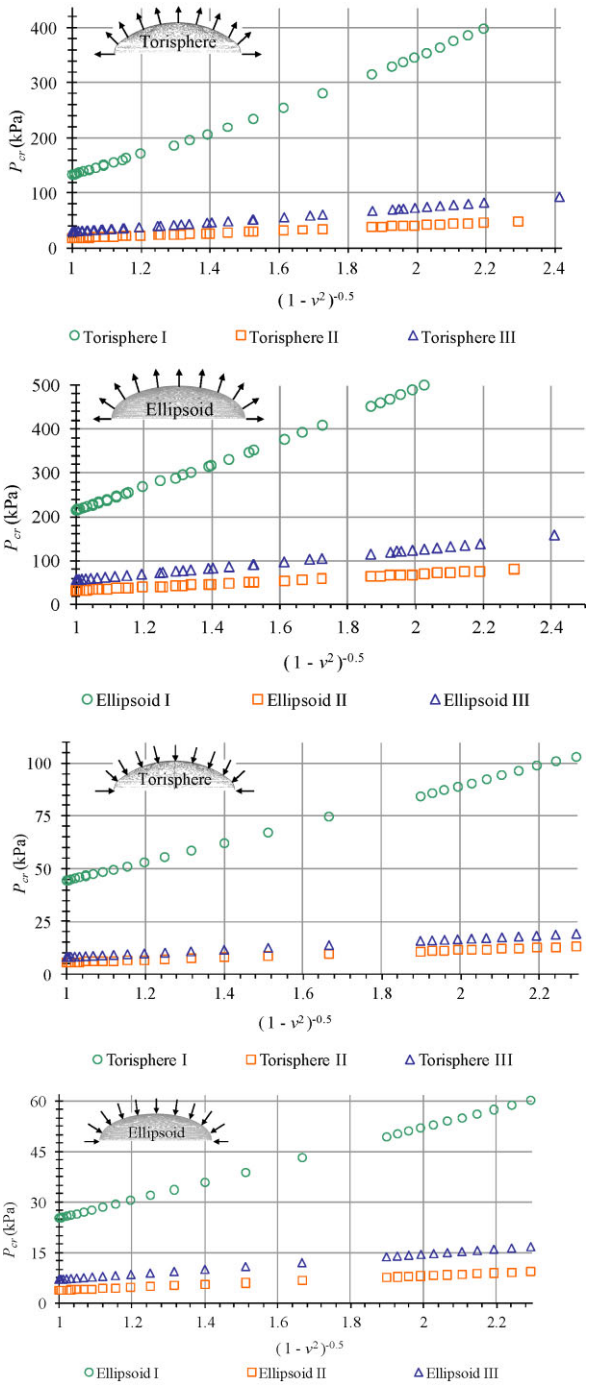

Figure 5 (online colour at: www.pss-b.com) Plots showing the relationship between the Poisson's ratio and the $(1-\nu^2)^{-1/2}$ fraction.

wavelengths for the torisphere and ellipsoid under internal pressure where the simulations suggest that for $\nu < -0.5$, and $\nu \to -1$, the amount of buckling wavelengths is observed to decrease. On the other hand, as illustrated in Fig. 6, the simulations suggest that the maximum transverse displacement/amplitude of these buckling wavelengths increase independently of the buckling mode. Similar characteristics in the buckling mode were observed by Obrecht et al. who modelled the buckling of axially compressed auxetic cylindrical shells thus adding more confidence to the validity of our results.

Table 2 Linear regression analysis of P_{cr} with $(1-\nu^2)^{-1/2}$ for various regions of ν for the torispheres under internal pressure.

Set	ν	m	R^2	m	c	R^2	n
I	0 to 0.5	134 615	0.9309	182 428	−50 289	0.9997	11
	−0.5 to 0	135 391	0.9101	193 269	−60 922	0.9999	11
	−1.0 to −0.5	254 174	0.7951	405 082	−419 861	0.9769	21
II	0 to 0.5	16 861	0.954	21 447	−4823	0.9998	11
	−0.5 to 0	16 948	0.9385	22 528	−5873	1	11
	−1.0 to −0.5	23 930	0.8905	33 037	−22 956	0.9887	29
III	0 to 0.5	29 801	0.9442	38 993	−9631	0.9998	11
	−0.5 to 0	29 989	0.9344	40 300	−10 902	1	11
	−1.0 to −0.5	36 881	0.9282	49 141	−23 463	0.9953	28

Table 3 Linear regression analysis of P_{cr} with $(1-\nu^2)^{-1/2}$ for various regions of ν for the torispheres under external pressure.

Set	ν	m	R^2	m	c	R^2	n
I	0 to 0.5	44 309	0.9990	44 090	228	0.9990	10
	−0.5 to 0	44 289	0.9992	43 659	664	0.9994	11
	−1.0 to −0.5	44 895	0.9996	45 472	−1907	0.9998	36
II	0 to 0.5	5691	0.9997	5716	−26	0.9997	10
	−0.5 to 0	5697	0.9992	5834	−144	0.9997	11
	−1.0 to −0.5	5800	0.9997	5875	−249	0.9999	36
III	0 to 0.5	8246	0.9983	8571	−338	0.9997	10
	−0.5 to 0	8252	0.9981	8617	−384	0.9999	11
	−1.0 to −0.5	8444	0.9994	8611	−553	0.9999	36

Table 4 Linear regression analysis of P_{cr} with $(1-\nu^2)^{-1/2}$ for various regions of ν for the ellipsoids under internal pressure.

Set	ν	m	R^2	m	c	R^2	n
I	0 to 0.5	215 666	0.9812	249 816	−35 918	0.9999	11
	−0.5 to 0	216 758	0.9656	266 020	−51 853	1	11
	−1.0 to −0.5	302 954	0.8763	427 903	−320 949	0.9873	27
II	0 to 0.5	31 314	0.9942	33 880	−2700	1	11
	−0.5 to 0	31 337	0.9931	34 170	−2982	1	11
	−1.0 to −0.5	38 463	0.9297	49 168	−26 983	0.9911	29
III	0 to 0.5	56 653	0.9921	62 147	−5788	1	10
	−0.5 to 0	56 716	0.9898	63 082	−6708	1	10
	−1.0 to −0.5	74 849	0.9547	89 687	−50 929	0.9918	37

Table 5 Linear regression analysis of P_{cr} with $(1-\nu^2)^{-1/2}$ for various regions of ν for the ellipsoids under external pressure.

Set	ν	m	R^2	m	c	R^2	n
I	0 to 0.5	215 666	0.9812	249 816	−35 918	0.9999	11
	−0.5 to 0	216 758	0.9656	266 020	−51 853	1	11
	−1.0 to −0.5	302 954	0.8763	427 903	−320 949	0.9873	27
II	0 to 0.5	31 314	0.9942	33 880	−2700	1	11
	−0.5 to 0	31 337	0.9931	34 170	−2982	1	11
	−1.0 to −0.5	38 463	0.9297	49 168	−26 983	0.9911	29
III	0 to 0.5	56 653	0.9921	62 147	−5788	1	10
	−0.5 to 0	56 716	0.9898	63 082	−6708	1	10
	−1.0 to −0.5	74 849	0.9547	89 687	−50 929	0.9918	37

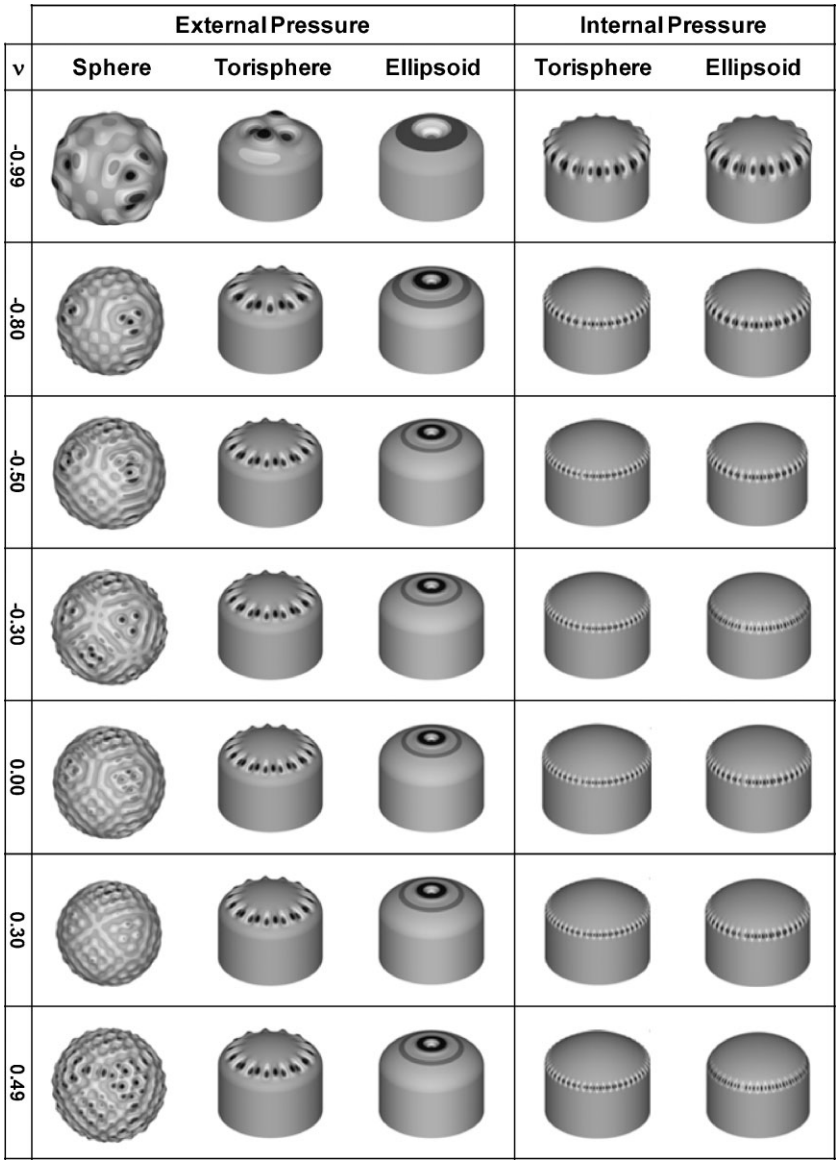

Figure 6 Contours showing the transverse displacements of the first eigenmode of some shells analysed.

Table 6 Number of circumferential wavelengths of the torisphere and ellipsoid with dimension set no. I.

ν	torisphere I	ellipsoid I
−0.99	18	16
−0.9	34	28
−0.8	40	32
−0.7	44	36
−0.6	46	38
−0.5	50	40
−0.3	52	44
0	52	44
0.3	52	42
0.49	50	40

6 Conclusions In this paper, we have shown through FE modelling that spherical, torispherical and ellipsoidal shells manufactured from isotropic auxetic materials having Poisson's ratio less than −0.5 benefit from enhanced resistance to buckling when subjected to internal (in the case of the torispheres and ellipsoids) or external pressures (in all cases). In particular, for all shapes, we found that to a first approximation, the critical buckling pressures scales linearly with $(1-\nu^2)^{-1/2}$ thus suggesting that the critical buckling pressures tends to infinity as ν tends to −1. All this is very significant, especially in view of the fact that it is envisaged that such shells can be manufactured with greater ease than those made from conventional materials in view of the enhanced ability of auxetics to adopt double curved shapes.

Acknowledgements Use of the ANSYS finite element software through an educational license is acknowledged.

References

[1] R. S. Lakes, Science **235**, 1038 (1987).
[2] F. Scarpa and F. C. Smith, J. Intel. Mater. Syst. Str. **15**(12), 973 (2004).
[3] K. E. Evans, M. A. Nkansah, I. J. Hutchinson, and S. C. Rogers, Nature **353**, 124 (1991).
[4] F. Scarpa and G. Tomlinson, J. Sound Vib. **230**(1), 45 (2000).
[5] L. J. Gibson, M. F. Ashby, G. S. Schajer, and C. I. Robertson, Proc. R. Soc. Lond. A **382**, 25 (1982).
[6] F. Scarpa, W. A. Bullough, and P. Lumley, P. I. Mech. Eng. C-J. Mech. Eng. Sci. **218**(2), 241 (2004).
[7] F. Scarpa, L. G. Ciffo, and J. R. Yates, Smart Mater. Struct. **13**(1), 49 (2004).
[8] R. F. Almgren, J. Elast. **15**(4), 427 (1985).
[9] D. Prall and R. S. Lakes, Int. J. Mech. Sci. **39**(3), 305 (1997).
[10] A. Spadoni, M. Ruzzene, and F. Scarpa, Phys. Status Solidi B **242**(3), 695 (2005).
[11] K. W. Wojciechowski, Mol. Phys. **61**(5), 1247 (1987).
[12] K. W. Wojciechowski and A. C. Brańka, Phys. Rev. A **40**(12), 7222 (1989).
[13] K. W. Wojciechowski, J. Phys. A: Math. Gen. **36**(47), 11765 (2003).
[14] C. B. He, P. W. Liu, P. J. McMullan, and A. C. Griffin, Phys. Status Solidi B **242**(3), 576 (2005).
[15] N. Gaspar, C. W. Smith, E. A. Miller, G. T. Seidler, and K. E. Evans, Phys. Status Solidi B **242**(3), 550 (2005).
[16] C. W. Smith, J. N. Grima, and K. E. Evans, Acta Mater. **48**(17), 4349 (2000).
[17] K. E. Evans and B. D. Caddock, J. Phys. D: Appl. Phys. **22**(12), 1883 (1989).
[18] B. D. Caddock and K. E. Evans, J. Phys. D: Appl. Phys. **22**(12), 1877 (1989).
[19] A. Alderson and K. E. Evans, J. Mater. Sci. **30**(13), 3319 (1995).
[20] R. H. Baughman and D. S. Galvão, Nature **365**(6448), 735 (1993).
[21] C. B. He, P. W. Liu, and A. C. Griffin, Macromolecules **31**(9), 3145 (1998).
[22] J. N. Grima and K. E. Evans, Chem. Commun. **16**, 1531 (2000).
[23] J. N. Grima, J. J. Williams, and K. E. Evans, Chem. Commun. **32**, 4065 (2005).
[24] G. Y. Wei, Phys. Status. Solidi B **242**(3), 742 (2005).
[25] R. H. Baughman, J. M. Shacklette, A. A. Zakhidov, and S. Stafstrom, Nature **392**(6674), 362 (1998).
[26] A. Yeganeh-Haeri, D. J. Weidner, and D. J. Parise, Science **257**(5070), 650 (1992).
[27] N. R. Keskar and J. R. Chelikowsky, Phys. Rev. B **46**(1), 1 (1992).
[28] H. Kimizuka, H. Kaburaki, and Y. Kogure, Phys. Rev. Lett. **84**(24), 5548 (2000).
[29] A. Alderson and K. E. Evans, Phys. Rev. Lett. **89**(22), 225503 (2002).
[30] H. Kimizuka, H. Kaburaki, and Y. Kogure, Phys. Rev. B **67**(2), 024105 (2003).
[31] G. N. Grima, R. Gatt, A. Alderson, and K. E. Evans, J. Mater. Chem. **15**, 4003 (2005).
[32] K. W. Wojciechowski, A. Alderson, K. L. Alderson, B. Maruszewski, and F. Scarpa, Phys. Status Solidi B **244**(3), 813 (2007).
[33] K. W. Wojciechowski, A. Alderson, A. Brańka, and K. L. Alderson, Phys. Status Solidi B **242**(3), 497 (2005).
[34] J. N. Grima and K. W. Wojciechowski, Phys. Status Solidi B **245**(11), 2369 (2008).
[35] C. W. Smith and K. W. Wojciechowski, Phys. Status Solidi B **245**(3), 486 (2008).
[36] F. Scarpa, C. W. Smith, M. Ruzzene, and M. K. Wadee, Phys. Status Solidi B **245**(3), 584 (2008).
[37] M. K. Wadee, M. A. Wadee, and A. P. Bassom, J. Mech. Phys. Solids **55**(5), 1086 (2007).
[38] D. Bushnell, Computerized analysis of shells. (Kluwer Academic Publishers, Hingham, Dordrecht, Boston, London, 1989).
[39] J. Singer and J. Arbocz, Basic concepts, columns, beams and plates, in: Buckling Experiments: Experimental Methods in Buckling of Thin Walled Structures, Vol. 1 (John Wiley & Sons, New York, 1997).
[40] R. V. Southwell, Philos. Trans. R. Soc. Ser. A **213**, 187 (1913).
[41] M. Biot, in: Proceedings of 5th International Congress on Applied Mechanics, Cambridge, USA, 1939, Part B (Wiley, New York, 1939), pp. 117–122.
[42] G. D. Galletly and R. W. Aylward, Int. J. Pres. Ves. Pip. **1**(2), 139 (1973).
[43] P. R. Patel and S. S. Gill, Int. J. Mech. Sci. **20**(3), 159 (1978).
[44] J. Sorić, Thin-Walled Struct. **23**(1-4), 57 (1995).
[45] A. Tafreshi, Int. J. Pres. Ves. Pip. **71**(1), 77 (1997).
[46] Y. Q. Ma, C. M. Wang, and K. K. Ang, Thin-Walled Struct. **46**(6), 584 (2008).
[47] J. Y. Han, H. Y. Jung, J. R. Cho, J. H. Choi, and W. B. Bae, J. Mater. Process. Tech. **201**(1-3), 742 (2008).
[48] G. D. Galletly, Stress failure of large pressure vessels – Recommendations resulting from studies of the collapse of a 68ft high × 45ft dia. pressure vessel, Tech. Report No 45-57, Shell Development Corp., Emeryville, California, 1957.
[49] S. P. Timoshenko and J. M. Gere, Theory of Elastic Stability, 2nd edition, (McGraw-Hill, Singapore, 1961), pp. 512–517.
[50] R. Zoelly, Über ein Knickungsproblem an die Kugelschale, Dissertation, Zürich, 1915.
[51] H. Obrecht, B. Rosenthal, P. Fuchs, S. Lange, and C. Marusczyk, Comput. Mech. **37**(6), 498 (2006).
[52] ANSYS® Academic Research, v. 11.0.
[53] C. D. Miller, R. B. Grove, and J. G. Bennett, Int. J. Pres. Ves. Pip. **22**(2), 147 (1986).
[54] G. D. Galletly and J. Blachut, Proc. Inst. Mech. Eng. Part C **199**(3), 225 (1985).
[55] R. J. Bellifante and R. R. Meyer, Fabrication and experimental evaluation of common domes having waffle-like stiffening. Part I – program development, Tech. Report No. NASA-CR-62257; SM-47742, PT. 1, Douglas Aircraft Company Inc., Santa Monica, California, 1964.

